Synthetic trimeric interleukin-6 receptor complexes with a STAT3 phosphorylation dominated activation profile

Christiane Seibel, Silke Pudewell, Puyan Rafii, Julia Ettich, Hendrik T. Weitz, Alexander Lang, Patrick Petzsch, Karl Köhrer, Doreen M. Floss, Jürgen Scheller

Suggested Citation:
Seibel, C., Pudewell, S., Rafii, P., Ettich, J., Weitz, H. T., Lang, A., Petzsch, P., Köhrer, K., Floß, D. M., & Scheller, J. (2024). Synthetic trimeric interleukin-6 receptor complexes with a STAT3 phosphorylation dominated activation profile. Cytokine, 184, Article 156766. https://doi.org/10.1016/j.cyto.2024.156766

Cytokine 184 (2024) 156766

Contents lists available at ScienceDirect

Cytokine

journal homepage: www.elsevier.com/locate/cytokine

Synthetic trimeric interleukin-6 receptor complexes with a STAT3 phosphorylation dominated activation profile

Christiane Seibel [a], Silke Pudewell [a], Puyan Rafii [a], Julia Ettich [a], Hendrik T. Weitz [a], Alexander Lang [b], Patrick Petzsch [c], Karl Köhrer [c], Doreen M. Floss [a], Jürgen Scheller [a,*]

[a] *Institute of Biochemistry and Molecular Biology II, Medical Faculty and University Hospital Düsseldorf, Heinrich-Heine-University Düsseldorf, Düsseldorf 40225, Germany*
[b] *Cardiovascular Research Laboratory, Medical Faculty and University Hospital Düsseldorf, Heinrich-Heine-University Düsseldorf, Düsseldorf 40225, Germany*
[c] *Biological and Medical Research Center (BMFZ), Medical Faculty and University Hospital Düsseldorf, Heinrich-Heine-University Düsseldorf, Düsseldorf 40225, Germany*

ARTICLE INFO

Keywords:
Interleukin 6
gp130
Janus kinase
synthetic cytokine biology

ABSTRACT

In Interleukin (IL)-6 signalling, IL-6 site I binds to the IL-6 receptor (IL-6R) first, following by IL-6 site II interaction to domain 2/3 of gp130 to form premature trimeric IL-6:IL–6R:gp130 receptor complexes. Formation of the mature hexameric receptor complex is then facilitated by the inter-trimeric interaction of IL-6 site III with domain 1 of the opposing gp130. The two gp130-associated Janus kinases (JAKs) *trans*-phosphorylate when their spatiotemporal pairing is correct, which causes the activation of STAT, ERK, and AKT pathways in a balanced manner. Since the intracellular domain (ICD) of IL-6R is not needed for STAT/ERK/AKT phosphorylation, we investigated the conditions under which a chimeric IL-6R_{ECD}-gp130$_{TMD/ICD}$ receptor protein confers biological activity. For IL–6R_{ECD}–gp130$_{TMD/ICD}$, the extracellular domain (ECD) of IL-6R was fused to the transmembrane domain (TMD) and ICD of gp130. Co-expression of IL–6R_{ECD}–gp130$_{TMD/ICD}$ with signalling-deficient gp130 variants did not induce IL-6 signalling, suggesting that the assembly of hexameric complexes failed to dimerize the IL-6R-associated JAKs correctly. By mimicking the premature trimeric receptor complex, IL-6-mediated dimerization of IL-6R_{ECD}-gp130$_{TMD/ICD}$ with the single-cytokine-binding variant gp130$_{\Delta D1}$ induced signalling. Of note, IL-6 signalling via these synthetic gp130$_{\Delta D1}$:IL-6R_{ECD}-gp130$_{TMD/ICD}$ complexes resulted predominantly in STAT3 phosphorylation. A STAT3-dominated profile was also observed after IL-6-induced signalling mediated by a JAK-deficient IL–6R_{ECD}–gp130$_{TMD/ICD\Delta JAK}$ variant in complex with the JAK-proficient but STAT/ERK/AKT-deficient gp130$_{JAK\Delta ICD}$ variant. Our data showed that effective ERK/AKT signalling could not be executed after intracellular domain swapping from gp130 to the IL-6R. Taken together, the chimeric IL-6R/gp130 receptor may be helpful in the creation of customized synthetic IL-6 signalling.

1. Introduction

Cytokines are intercellular mediators regulating immunological responses, hematopoiesis, acute phase reactions, and non-inflammatory processes, including energy homeostasis or fertility [1]. They trigger receptor dimerization or oligomerization by binding to particular cell surface receptors on their intended target cells [2]. The intracellular signal transduction cascade is started, which involves the phosphorylation of signalling proteins and transcription factors and which subsequently causes the cytoplasmic portions of the corresponding receptors to juxtapose [2]. The major immunomodulatory cytokine, Interleukin-6 (IL-6), influences the course of several illnesses, such as cancer, autoimmune diseases, and chronic inflammatory diseases. The signal transducing receptor of IL–6 is the β-receptor gp130. The intracellularly associated tyrosine kinases of the Janus kinase (JAK) family members JAK1, JAK2, and TYK2 are activated upon gp130 homodimerization. Subsequently, these kinases phosphorylate tyrosine residues in the cytoplasmic portion of the signal transducer gp130 [3,4], as a result, these residues serve as docking sites for signal transducer and activators of transcription (STAT) factors. Moreover, binding of SHP2 (SHP) initiates AKT and MAPK signalling pathways [5,6]. Suppressor of cytokine signalling 3 (SOCS3) is one of the STAT3 target genes that acts as

* Corresponding author.
E-mail address: jscheller@uni-duesseldorf.de (J. Scheller).

https://doi.org/10.1016/j.cyto.2024.156766
Received 7 August 2024; Received in revised form 11 September 2024; Accepted 18 September 2024
Available online 29 September 2024

negative feedback regulator of IL-6 signalling [7]. In IL-6 *trans*-signalling, IL-6 in complex with soluble IL-6 receptor α (IL-6R) activate gp130 resulting in signalling that has generally overlapping characteristics with classic IL-6 signalling, which is mediated by IL-6:membrane-bound IL-6R:gp130 complexes [8,9]. Of note, the intracellular domain (ICD) of IL–6R has neither a binding site for JAKs nor binding sites to facilitate any signalling. Therefore, the IL-6R is considered as non-signal-transducing and rather IL–6–transforming receptor for interacting with gp130. The intracellular domain of IL-6R controls, however, basolateral sorting of the receptor on the cell surface [10,11].

The extracellular part of gp130 comprises the N-terminal Ig-like domain (domain 1), followed by the cytokine binding module (CBM, domains 2 and 3) and three fibronectin type three-like (FN3) domains (domains 4–6). The binding of IL-6 to gp130 depends on prior binding to the IL-6R, which consists of three extracellular domains, followed by a flexible stalk region, a transmembrane domain, and an intracellular domain [12,13]. Like IL-6, the IL-6R alone did not bind to gp130 [10]. IL-6 has three receptor binding sites. Initial recruitment of IL-6R is mediated by site I, whereas subsequent gp130 complexing is mediated by binding interfaces site II and site III of IL-6 [14–16]. At least two different biologically active receptor assemblies are conceivable, and experimental data suggest the formation of tetrameric IL-6:IL-6R:$(gp130)_2$ or hexameric $(IL\text{-}6)_2$:$(IL\text{-}6R)_2$:$(gp130)_2$ receptor complexes [9]. Accordingly, two different hypotheses explain the sequence resulting in the formation of the receptor complexes.

First, the IL-6:IL-6R complex recruits one gp130 receptor via site II interaction and, subsequently, a second gp130 receptor via site III interaction to form an intermediate tetrameric receptor complex. A second IL-6:IL-6R complex is later recruited to form the hexameric complex [17]. The proposed tetrameric IL-6:IL-6R:$(gp130)_2$ receptor complex is considered biologically active, leading to the hypothesis that the change from tetrameric to hexameric states may act as a molecular switch between active and inactive receptor complexes or may cause different signalling strength and quality [18].

In the alternative and experimentally supported hypothesis, premature, trimeric IL–6:IL–6R:gp130 complexes form the interaction of IL-6 site II and the CBM of gp130 (domain 2 and 3). This trimeric receptor complex is not active. Two trimeric complexes form the mature hexameric receptor signalling complex via the inter-trimeric binding site III of IL-6 and gp130 Ig-like domain 1 [14,19–22]. In short, physiologically inert trimeric receptor complexes are directly transformed into biologically active hexameric receptor complexes [14] (Supplemental Fig. 1).

Here, we generated a series of chimeric IL-6 type receptors and deletion variants as tools to understand receptor complex formation and *trans*-phosphorylation on living cells. Our data revealed that the chimeric $IL\text{-}6R_{ECD}$-$gp130_{TMD/ICD}$ receptor induced customized synthetic IL-6 signalling.

2. Material and Methods

2.1. Cloning

cDNAs coding for IL-6R and gp130 were described previously [23]. The cDNA coding for C-terminally HA-tagged $IL\text{-}6R_{ECD}gp130_{TMD,ICD}$ comprised the amino acids 1–365 of IL-6R and 620–918 of gp130 and was generated by splicing by overlap extension polymerase chain reaction (SOE-PCR). $gp130_{GPI}$ cDNA codes for the complete extracellular domain from amino acids 1 to 619 of gp130 fused to the glycosylphosphatidylinositol (GPI)-anchor sequence from the human alkaline phosphatase precursor (YTACDLAPPAGTTDAAHPGRSVVPALLPLLAGTLLLLE TATAPS) [24] and was generated by PCR. cDNAs coding for $gp130_{\Delta ICD}$ containing the amino acids 1 to 651 and $gp130_{\Delta D1}$ lacking the D1 domain amino acids from 23 to 124 and $gp130_{JAK\Delta ICD}$ containing the amino acids 1 to 699 were all generated by PCR using Q5 Site-Directed Mutagenesis Kit (New England Biolabs GmbH). The point mutations in the cDNAs coding for the receptor variants $gp130_{Y190K/F191E}$, $IL\text{-}6R_{ECD}gp130_{TMD,ICD\Delta JAK}$ (containing the amino acid exchanges P399V, P402V, P404V) were generated by site-directed mutagenesis. The cDNAs coding for the three dimeric VHH6-Linker-Fc variants [25,26] contained rigid linkers of composed $(EAAAK)_2$, $(EAAAK)_8$ or $(EAAAK)_{12}$ [27] and were generated by primer ligation. Primer sequences will be provided upon request. All cDNAs were verified by sequencing and cloned into pcDNA3.1 and/or pMOWS plasmids. For retroviral transduction of Ba/F3 cells, the plasmids pMOWS-puro with puromycin resistance gene [28], and pMOWS-hygro with hygromycin B resistance gene were used for subcloning [29].

2.2. Cells, reagents and recombinant proteins

The generation of Ba/F3-gp130 and Ba/F3-gp130:IL-6R cells was described elsewhere [23]. The packaging cell line Phoenix-Eco was received from Ursula Klingmüller (DKFZ, Heidelberg, Germany). All cells were grown at 37 °C with 5 % CO_2 in a water-saturated atmosphere in Dulbecco's modified Eagle's medium (DMEM) high-glucose culture medium (GIBCO®, Life Technologies, Darmstadt, Germany) with 10 % fetal calf serum (GIBCO®, Life Technologies) and 60 mg/l penicillin and 100 mg/l streptomycin (Genaxxon Bioscience GmbH, Ulm, Germany). Proliferation was maintained in Ba/F3 cells by adding 0.2 % conditioned medium of WEHI-3B cells [IL-3 (10 ng/mL)] (DSMZ ACC-26). Ba/F3-gp130 cells or variants thereof were maintained in the presence of HIL-6, a fusion protein of IL-6 and the sIL-6R, which mimics IL-6 *trans*-signalling [30]. Either recombinant protein (10 ng/mL) or conditioned cell culture medium from a stable CHO-K1 clone secreting HIL-6 (10 ng/mL) was used [30]. Expi-293F™ cells (ThermoFisher Scientific) were cultured in Expi293™ expression medium without antibiotics until they reached a density of 3–5 × 10^6 cells/ml in a 37 °C incubator with 8 % CO_2 on an orbital shaker at 125 rpm. Cytokines and VHH6Fc fusion proteins were expressed and purified as described [10,26,31].

2.3. Stimulation assay

Ba/F3 cell lines were washed three times with PBS to remove cytokines and starved in serum-free DMEM for 4 h. Cells were stimulated for 20 min with the indicated cytokines, harvested, frozen in liquid nitrogen and then lysed at 4 °C for 1 h with buffer containing 10 mM Tris-HCl, pH 7.5, 150 mM NaCl, 0.5 mM $MgCl_2$ and a cOmplete, EDTA-free protease inhibitor mixture tablet (Roche Diagnostics, Mannheim, Germany). Protein concentration was determined by a BCA protein assay (Thermo Fisher Scientific) according to the manufacturer's instruction.

2.4. Western blottin

For fluorescence-based Western blotting: 50 µg total protein were loaded on each lane and separated by SDS-PAGE under reducing conditions and transferred to a nitrocellulose membrane (Amersham Protan; Cytiva; LC, United Kingdom; catalogue no. 10600016). Blocking of membrane was performed with blocking buffer (Intercept® blocking buffer; LI–COR; USA; catalogue no. 927–60001) diluted 1:3 in TBS (10 mM Tris-HCl pH 7.6, 150 mM NaCl) for 1 h. Primary antibodies phospho-STAT3, Tyr-705, catalogue no. 9145; STAT3, catalogue no. 9139; ERK1/2, catalogue no. 4696; phospho-ERK1/2, catalogue no. 4370; AKT, catalogue no. 9272; phospho-AKT, catalogue no. 4060 were incubated at 4 °C overnight. Membranes were washed with TBS-T (0.1 % Tween-20) and then incubated with secondary fluorophore-conjugated antibodies 1:10,000 (For IRDye® 800CW donkey anti-rabbit, catalogue no. 926–32213 or IRDye® 680RD donkey anti-mouse, catalogue no. 926–68072; for LI-COR; USA or with IRDye 800CW donkey anti-goat, catalogue no. 926–32214) for 1 h. Signal detection was achieved using LI-COR Odyssey (USA; Model 2800). Secondary antibodies were detected simultaneously on different channels. Data analysis was conducted using Image Studio Lite 5.2.

For chemiluminescence-based Western blotting: 50 µg total protein

was separated by SDS-PAGE and transferred to polyvinylidene fluoride (PVDF) membranes. Membranes were blocked in 5 % milk solution /milk blocking buffer for 2 h (2.5 g milk powder diluted in 50 mL TBS-T (0.05 % Tween20) and probed with the primary antibodies (JAK1 (6G4) catalogue no. 3344 and p-JAK1$^{Y1034/1035}$ catalogue no. 3331 (Cell Signaling Technology, USA), CIS3/SOCS3, catalogue no.C204 (IBL-America, USA)). After washing, membranes were incubated with secondary peroxidase-conjugated antibodies (Pierce (Thermo Fisher Scientific)) in BSA 5 % (2.5 g BSA diluted in 50 mL TBS-T (0.05 % Tween20) (BSA: Bovin Serum albumin fraction V, IgG-free, US-Origin, 500 g, Carl Roth, CAS NR. 9048–46-8). The Immobilon™ Western Reagents (Millipore Corporation, Billerica, MA, USA) and the ChemoCam Imager (INTAS Science Imaging Instruments GmbH, Göttingen, Germany) were used for signal detection.

2.5. Cell viability assay

Ba/F3 cell lines were washed three times with PBS to remove cytokines from the medium. Cells with a density of 5x10^4 cells/mL were suspended in DMEM containing 10 % fetal calf serum, 60 mg/l penicillin and 100 mg/ml streptomycin. Cells were cultured for 3 days in a volume of 100 µl with the indicated cytokines/proteins. The CellTiter blue viability assay (Promega, Karlsruhe, Germany) was used to estimate the approximate number of viable cells by measuring the fluorescence ($\lambda_{excitation}$560 nm/$\lambda_{emission}$590 nm) using the Infinite M200 Pro plate reader (Tecan, Crailsheim, Germany). After adding 20 µl/well of CellTiter blue reagent (time point 0), fluorescence was measured every 20 min for up to 2 h. Each condition was determined in triplicates. All values were normalized by subtracting time point 0 values from the final measurement.

2.6 Transduction of cells. Ba/F3 cell lines were retrovirally transduced with the pMOWS expression plasmids as described [33]. Transduced cells were grown in DMEM medium as described above supplemented with IL-3 or HIL-6. Selection of transduced Ba/F3 cells was performed with puromycin (1.5 µg/ml) or hygromycin B (1 mg/ml) (Carl Roth, Karlsruhe, Germany) for at least 2 weeks. Afterwards, the generated Ba/F3 cell lines were analyzed for receptor cell surface expression via flow cytometry.

2.6. Cell surface detection of cytokine receptors via flow cytometry

Cell surface expression of proteins in stably transfected Ba/F3 cells was detected flow cytometry. 5×10^5 cells were washed in FACS buffer (PBS, 1 % BSA) and then incubated in 50 µl of FACS buffer containing the indicated specific primary antibody (1:50 dilution anti-IL-6R (4–11 [32]) and 1:50 dilution anti-gp130 (B-R3, ab34315, Abcam, Cambridge, UK). After incubation for 1 h at room temperature, cells were washed and resuspended in 50 µl of FACS buffer containing secondary antibody (NothernLights 493–conjugated anti-goat IgG, 1:100) and incubated for 1 h at room temperature. Cells were washed and resuspended in 500 µl of FACS buffer and analyzed by flow cytometry (BD FACSCanto II flow cytometer using the FACSDiva software, BD Biosciences). Data analysis was conducted using FlowJo Version 10 (Tree Star Inc, US).

2.7. RNA-seq analyses

Ba/F3-gp130$_{JAK\Delta ICD}$:IL-6R$_{ECD}$-gp130$_{TMD,ICD}$ cells were stimulated with IL-6 for 40 min at 37 °C with the indicated cytokines (100 ng/mL). mRNA was isolated with NucleoSpin RNA (Macherey-Nagel, Düren, Germany; cat. no. 740955.250) according to vendor's manual. DNase digested total RNA samples used for 3́-RNA-Seq analyses were quantified (Qubit RNA HS Assay, Thermo Fisher Scientific) and quality measured by capillary electrophoresis using the Fragment Analyzer and the 'Total RNA standard Sensitivity Assay' (Agilent Technologies, Inc. Santa Clara, USA). All samples in this study showed a very high-quality RNA Quality Numbers (RQN; mean = 10.0). The library preparation was performed according to the manufacturer's protocol using the QuantSeq 3′ mRNA-Seq Library Prep Kit FWD from Lexogen®. Input mount was 100 ng of total RNA. Bead purified libraries were normalized and finally sequenced on the NextSeq2000 system (Illumina Inc. San Diego, USA) with a read setup of SR 1x100 bp. The Illumina DRAGEN FASTQ Generation tool (version 3.8.4) was used to convert the bcl files to fastq files as well for adapter trimming and demultiplexing. The gene ontology analysis was performed with the r package clusterprofiler and r version 4.1.3. Data analyses on fastq files were conducted with CLC Genomics Workbench (version 22.0.2, QIAGEN, Venlo. NL). After UMI (Unique Molecular Identifier) filtering, all remaining reads of all probes were adapter trimmed and quality trimmed (using the default parameters: bases below Q13 were trimmed from the end of the reads. After grouping of samples (for biological replicates each) according to their respective experimental condition, the statistical differential expression was determined using the Differential Expression for RNA-Seq tool (version 2.7). The resulting p values were corrected for multiple testing by FDR correction. A p value of ≤ 0.05 was considered significant. The Gene Set Enrichment Test (version 1.2) was done with default parameters. The lollipop-plot was created by filtering the GO term output for significance and unique genes, focusing on terms related to 'MAPK, STAT, ERK, Immunology, Apoptotic Tyrosine Kinase, JAK'.

2.8. Statistical analysis

Data are provided as arithmetic means ± SD using GraphPad Prism, Version 8. Statistically significant differences between two groups for quantification of Western blots were determined with a Students's *t*-test, including Welch's correction if indicated. Statistically analysis for qPCR between several groups were determined using a two-way ANOVA, including Tukey or Dunnet's correction. Significance was calculated as follows $p > 0.05$: n.s.; $p < 0.05$: *; $p < 0.01$: **; $p < 0.001$: ***; $p < 0.0001$: ****.

2.9. Data availability

The authors declare that the data supporting the findings of this study are available within the manuscript and from the authors on request. RNA-Seq data are deposited with the accession number: GSE267270.

3. Results

3.1. Transfer of the intracellular signalling domain of gp130 to IL-6R in the synthetic receptor IL–6R$_{ECD}$gp130$_{TMD/ICD}$ did not induce signalling after stimulation with IL-6

The hexameric assembly mode of the (IL-6)$_2$:(sIL-6R)$_2$:(sgp130)$_2$ complex, requires the recruitment of two IL-6R molecules in the final receptor complex. We questioned whether the intracellular signalling domain of gp130 could transduce signalling if transferred to the IL-6R as an intracellular substitute. In the chimeric receptor IL-6R$_{ECD}$gp130$_{TMD/ICD}$, the complete extracellular domain (ECD) of IL-6R was fused to the transmembrane domain (TMD) and intracellular domain of gp130 (Fig. 1A). Ba/F3 cells stably expressing IL-6R$_{ECD}$gp130$_{TMD/ICD}$ were generated, and expression of IL-6R$_{ECD}$gp130$_{TMD/ICD}$ on the cell surface was shown by flow cytometry (Supplemental Fig. 2A). Ba/F3-IL-6R$_{ECD}$gp130$_{TMD/ICD}$ cells were stimulated with increasing concentrations of IL-6 (10–10.000 ng/mL), which did not induce STAT3 and ERK phosphorylation (Fig. 1B). We expected that the chimeric IL-6R$_{ECD}$gp130$_{TMD/ICD}$ receptor did not signal after stimulation with IL-6 because the IL-6R harbours only one IL-6 binding site, and IL-6 was not shown to form dimers, therefore cross-linking of two IL-6R$_{ECD}$gp130$_{TMD/ICD}$ receptors was not expected. As controls, Ba/F3 and Ba/F3-gp130:IL-6R cells were stimulated with increasing concentrations of IL-6 (10–1.000 ng/mL) (Fig. 1C-E). As described previously, Ba/F3-

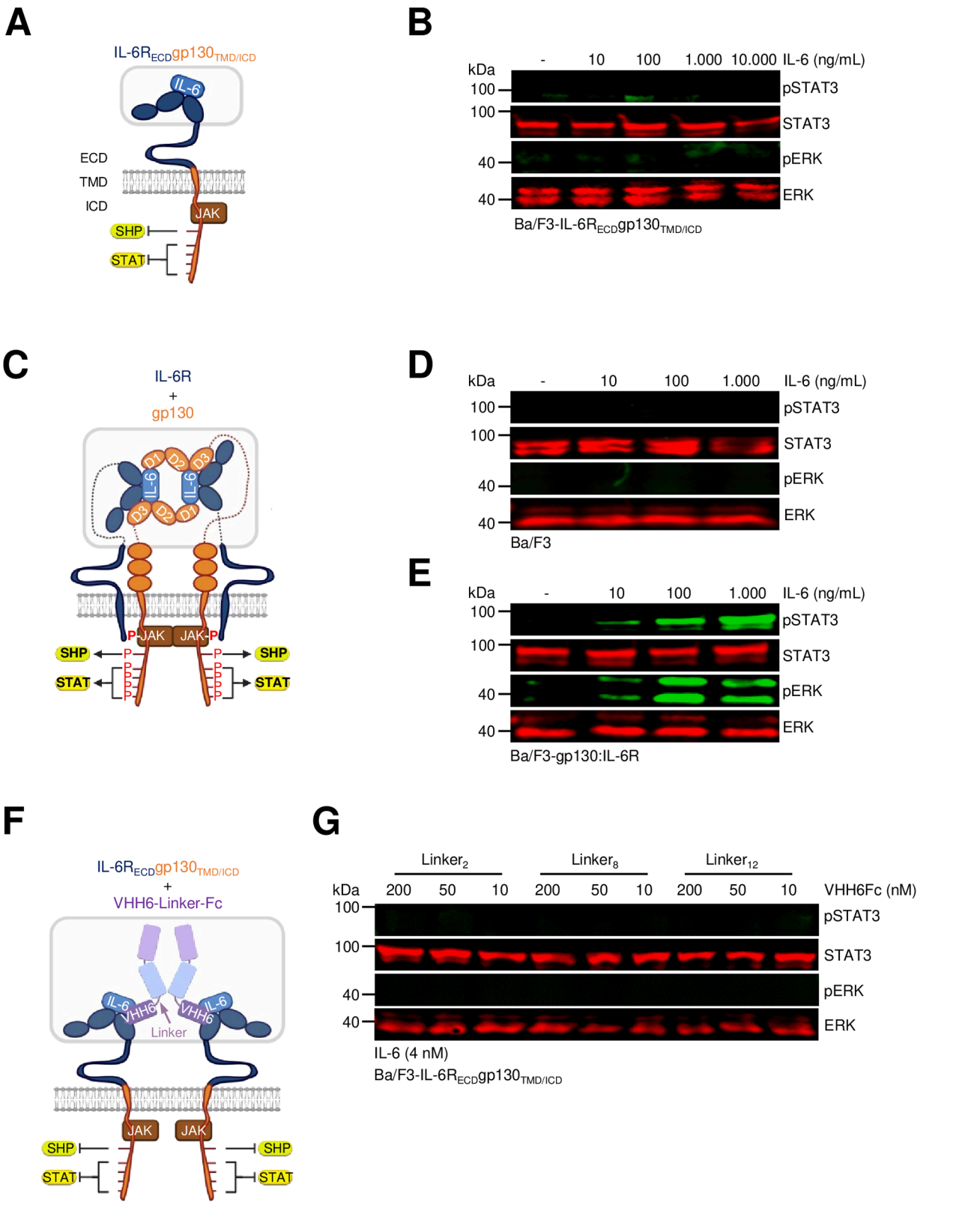

(caption on next page)

Fig. 1. Transfer of the intracellular signalling domain of gp130 to IL-6R in the synthetic receptor IL–6R$_{ECD}$gp130$_{TMD/ICD}$ did not induce signalling after stimulation with IL-6. (A) Schematic illustration of the receptor complex of IL-6 and IL–6R$_{ECD}$gp130$_{TMD/ICD}$. Signalling was not expected because IL-6 interacts with IL-6R via site I and does not form dimers. (B) STAT3 and ERK phosphorylation in Ba/F3-IL–6R$_{ECD}$gp130$_{TMD/ICD}$ cells without cytokine (−), and with 10, 100, 1.000, 10.000 ng/mL IL-6. Equal amounts of proteins (50 μg/lane) were analyzed via specific antibodies detecting phospho-STAT3, STAT3, phospho-ERK and ERK. Western blot data shows one representative experiment out of three. (C) Schematic illustration of the receptor complex of IL-6, IL-6R and gp130. Signalling was initiated by IL-6. (D) STAT3 and ERK phosphorylation in Ba/F3 cells without cytokine (−), and with 10, 100 and 1.000 ng/mL IL-6. Equal amounts of proteins (50 μg/lane) were analyzed via specific antibodies detecting phospho-STAT3, STAT3, phospho-ERK and ERK. Western blot data shows one representative experiment out of three. (E) STAT3 and ERK phosphorylation in Ba/F3-gp130:IL-6R cells without cytokine (−), and with 10, 100 and 1.000 ng/mL IL-6. Equal amounts of proteins (50 μg/lane) were analyzed via specific antibodies detecting phospho-STAT3, STAT3, phospho-ERK and ERK. Western blot data shows one representative experiment out of three. (F) Schematic illustration of the receptor complex of IL-6 and IL–6R$_{ECD}$gp130$_{TMD/ICD}$ in the presence of VHH6-Linker-Fc variants. (G) STAT3 and ERK phosphorylation in Ba/F3-IL–6R$_{ECD}$gp130$_{TMD/ICD}$ cells with 100 ng/mL (4 nM) IL-6 and 200, 50, 10 nM VHH6-Linker$_2$Fc, VHH6-Linker$_8$Fc and VHH6-Linker$_{12}$Fc. Equal amounts of proteins (50 μg/lane) were analyzed via specific antibodies detecting phospho-STAT3, STAT3, phospho-ERK and ERK. Western blot data shows one representative experiment out of three.

gp130:IL-6R but not Ba/F3 cells showed dose-dependent induction of STAT3 and ERK phosphorylation (Fig. 1D, E). Next, we aimed to induce IL-6R$_{ECD}$gp130$_{TMD/ICD}$ dimerization on the surface of Ba/F3 cells. We engineered a dimeric IgG1-Fc-fusion protein with the single domain antibody VHH6 that specifically interacts with IL-6:IL-6R complexes but not with IL-6 or IL-6R alone [25,33]. Three dimeric VHH6Fc variants were generated with various lengths of linker peptides connecting VHH6 and the Fc part. The linker peptide consists of two, eight or twelve repeats of the rigid amino acid sequence EAAAK which should allow different spacings of two IL-6R$_{ECD}$gp130$_{TMD/ICD}$ receptors (Fig. 1F). Dimeric VHH6Fc variants were expressed in Expi293-F^{TM} cells and purified via Protein A affinity chromatography (Supplemental Fig. 2B). VHH6Fc was biologically active because it enhanced IL-6 *trans*-signalling by forcing IL-6 into IL-6:sIL6R *trans*-signalling complexes as shown previously [25,33]. Only VHH6 fusion protein with the (EAAAK)$_2$-Linker was significantly more active by using 1.56–12.5 ng/mL IL-6 compared to the control without VHH6, indicating the importance of spacer length for the signal enhancement (Supplemental Fig. 2C). Accordingly, Ba/F3–IL–6R$_{ECD}$gp130$_{TMD/ICD}$ cells were stimulated with constant amounts of IL-6 (4 nM, 100 ng/mL) and increasing concentrations of the VHH6Fc variants (10–200 nM), which, however, did not induce STAT3 and ERK phosphorylation (Fig. 1G). We can only hypothesize why IL-6 plus VHH6Fc did not cause IL-6R$_{ECD}$gp130$_{TMD/ICD}$ to signal. Firstly, it is possible that VHH6Fc does not recruit two IL-6R$_{ECD}$gp130$_{TMD/ICD}$ proteins at the same time or that the induced receptor dimerization did not result in the IL-6R$_{ECD}$gp130$_{TMD/ICD}$ proteins being closely juxtaposed to trigger intracellular signalling.

3.2. Co-expression of the synthetic receptor of IL-6R$_{ECD}$gp130$_{TMD/ICD}$ with gp130 confers biological activity after stimulation with IL-6

To analyze if IL-6R$_{ECD}$gp130$_{TMD/ICD}$ can still bind and correctly present IL-6 to gp130, we co–expressed IL-6R$_{ECD}$gp130$_{TMD/ICD}$ with gp130 in Ba/F3 cells (Fig. 2A, Supplemental Fig. 3A). Stimulation of Ba/F3-gp130:IL-6R$_{ECD}$gp130$_{TMD/ICD}$ cells with IL-6 induced canonical STAT3 and ERK phosphorylation starting at concentrations of 10 ng/mL, demonstrating that IL–6R$_{ECD}$gp130$_{TMD/ICD}$ can bind to IL-6 and form biologically active complexes with gp130 (Fig. 2B). In this setting, however, it is not possible to distinguish between signalling initiated from the ICD of gp130 or IL-6R$_{ECD}$gp130$_{TMD/ICD}$. Moreover, this experiment did not address the question, whether signalling is initiated from tetrameric IL-6:IL-6R:(gp130)$_2$ or hexameric (IL-6)$_2$:(IL-6R)$_2$:(gp130)$_2$ complexes. To elucidate if signalling can be initiated from the ICD of IL-6R$_{ECD}$-gp130$_{TMD/ICD}$, we generated two signalling-incompetent deletion variants of gp130, which were co-expressed together with IL-6R$_{ECD}$gp130$_{TMD/ICD}$. In other words, the primary goal in this setting was to define if gp130 and the ECD of IL-6R$_{ECD}$gp130$_{TMD/ICD}$ could form a signal-transducing complex. Both variants, gp130$_{\Delta ICD}$, and gp130$_{GPI}$, lacked the complete intracellular domain. In gp130$_{\Delta ICD}$, only ten intracellular amino acids were retained [34], and in gp130$_{GPI}$, a glycosylphosphatidylinositol (GPI)-attachment signal [35] was placed at the C-terminal end of the extracellular domains of gp130 (Fig. 2C, D). Both receptors were expressed on the surface of Ba/F3 cells, as shown by flow cytometry (Supplemental Fig. 3B, C). Due to the lack of the intracellular domain in gp130$_{\Delta ICD}$ and gp130$_{GPI}$, Hyper IL-6 (HIL-6) stimulation failed to induce STAT3 phosphorylation in Ba/F3-gp130$_{\Delta ICD}$ and Ba/F3-gp130$_{GPI}$ cells (Fig. 2E, F). HIL-6 is a synthetic IL-6 *trans*-signalling agonist and was constructed by fusion of IL-6 and the soluble IL-6R connected by a flexible peptide linker [30]. Co-transduction of the cDNA coding for IL–6R$_{ECD}$gp130$_{TMD/ICD}$ into Ba/F3-gp130$_{\Delta ICD}$ and Ba/F3-gp130$_{GPI}$ cells might render these cells responsive to IL-6, at least if two IL-6R$_{ECD}$gp130$_{TMD/ICD}$ molecules are recruited into hexameric complexes (Supplemental Fig. 3D, E). As shown in Fig. 2G, H, STAT3 and ERK phosphorylation was not detected in Ba/F3-gp130$_{\Delta ICD}$:IL-6R$_{ECD}$gp130$_{TMD/ICD}$ and Ba/F3–gp130$_{GPI}$:IL-6R$_{ECD}$gp130$_{TMD/ICD}$ cells after stimulation with increasing amounts of IL-6 from 1 to 10.000 ng/mL. The absence of phosphorylation on STAT3 and ERK may counteract the creation of hexameric complexes but it is also possible that dimerization of IL–6R$_{ECD}$gp130$_{TMD/ICD}$ did not lead to the correct juxtaposition of the receptors to intracellular signalling.

3.3. Limited domain exchange of the intracellular domain of gp130 to the IL-6R enabled cross-receptor phosphorylation

The failure of gp130$_{GPI}$:IL-6R$_{ECD}$gp130$_{TMD/ICD}$ and gp130$_{\Delta ICD}$:IL-6R$_{ECD}$gp130$_{TMD/ICD}$ to generate signal transduction in Ba/F3 cells in response to IL-6 may also indicate the non-functionality of the gp130 intracellular domain fused to the IL-6R. Therefore, we separated JAK activation from receptor tyrosine phosphorylation and STAT/ERK phosphorylation in gp130$_{JAK\Delta ICD}$ and IL-6R$_{ECD}$gp130$_{TMD/ICD\Delta JAK}$ (Fig. 3A), which were both expressed alone or together on the surface of Ba/F3 cells (Supplemental Fig. 4A–C). gp130$_{JAK\Delta ICD}$ had a truncation of the intracellular domain of gp130 after the box 1 and box 2 motifs, which are crucial for JAK binding and activation [36]. IL-6R$_{ECD}$gp130$_{TMD/ICD\Delta JAK}$ deviated from IL to 6R$_{ECD}$gp130$_{TMD/ICD}$ by the amino acid exchanges P399V, P402V and P404V within the box 1 motif resulting in a complete inability to bind JAKs [34]. As expected, stimulation of Ba/F3-gp130$_{JAK\Delta ICD}$ cells with HIL-6, and of Ba/F3–IL-6R$_{ECD}$gp130$_{TMD/ICD\Delta JAK}$ with IL-6 failed to induce STAT and ERK signalling (Fig. 3B, C). Stimulation of Ba/F3-gp130$_{JAK\Delta ICD}$:IL-6R$_{ECD}$gp130$_{TMD/ICD\Delta JAK}$ cells with IL-6, however, resulted in phosphorylation of STAT3, whereas ERK was not phosphorylated even at concentrations as high as 1.000 ng/mL of IL-6 (Fig. 3D). Since ERK and AKT phosphorylation is initiated from the same phosphorylated tyrosine Y759 in the intracellular domain of gp130, we also showed that AKT was not phosphorylated (Fig. 3D). A time-dependent stimulation of Ba/F3-gp130$_{JAK\Delta ICD}$:IL-6R$_{ECD}$gp130$_{TMD/ICD\Delta JAK}$ cells with a fixed concentration of 100 ng/mL IL–6 demonstrated that STAT3 activation pattern of Ba/F3-gp130$_{JAK\Delta ICD}$:IL-6R$_{ECD}$gp130$_{TMD/ICD\Delta JAK}$ cells was comparable to Ba/F3-gp130:IL-6R cells. ERK phosphorylation was, however, not induced in Ba/F3-gp130$_{JAK\Delta ICD}$:IL-6R$_{ECD}$gp130$_{TMD/ICD\Delta JAK}$ cells during the complete stimulation time of 8 h (Fig. 3E). We noticed that at any time point, STAT3 phosphorylation was slightly (albeit not significantly) lower in Ba/F3-gp130$_{JAK\Delta ICD}$:IL-6R$_{ECD}$gp130$_{TMD/ICD\Delta JAK}$ cells compared

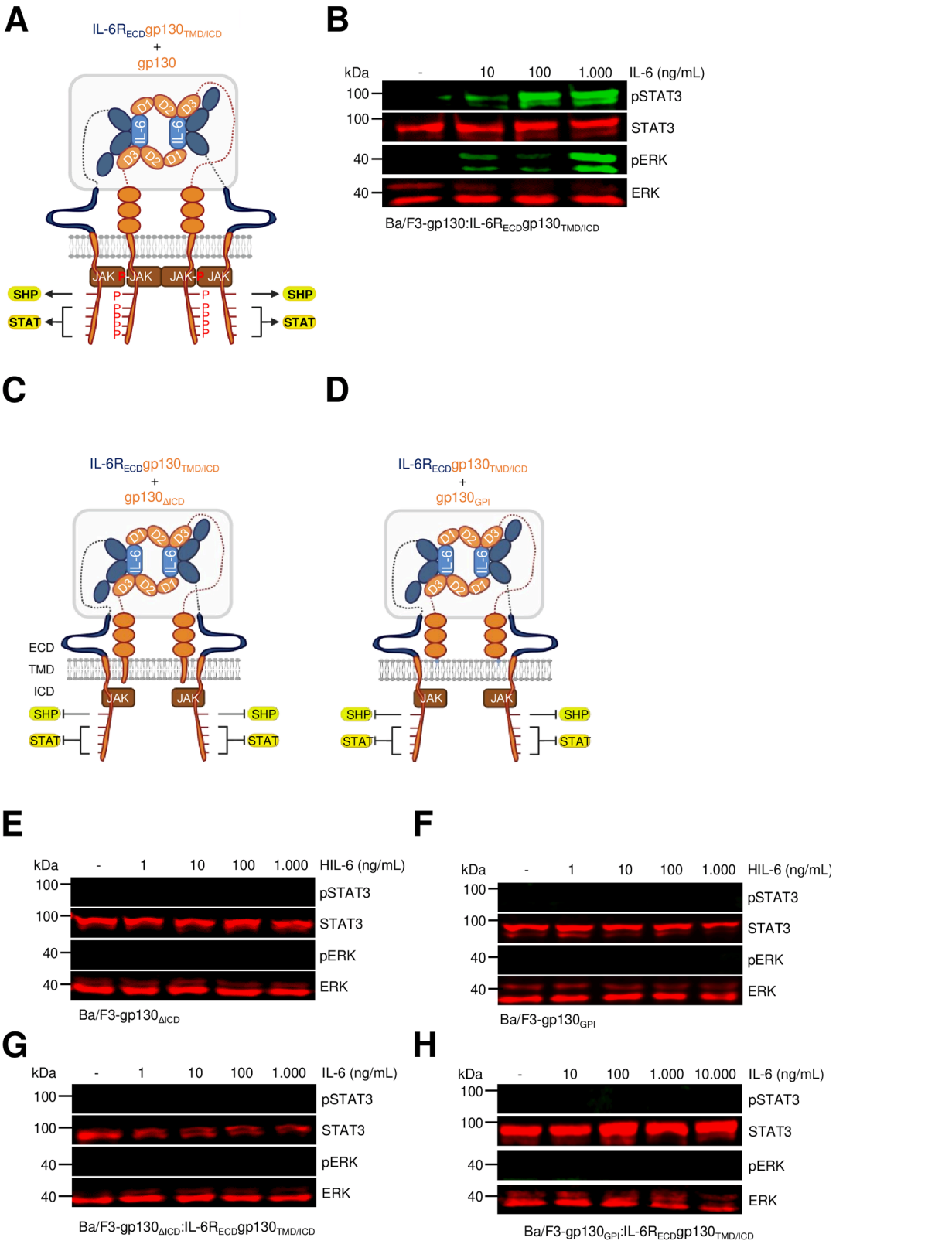

(caption on next page)

Fig. 2. Co-expression of the synthetic receptor of IL-6R_{ECD}gp130$_{TMD/ICD}$ with gp130 confers biological activity after stimulation with IL-6. (A) Schematic illustration of the receptor complex of IL-6, IL–6R_{ECD}gp130$_{TMD/ICD}$ and gp130. Signalling was expected because IL-6 interacts with IL-6R via site I and via site II/III with gp130. (B) STAT3 and ERK phosphorylation in Ba/F3-gp130:IL–6R_{ECD}gp130$_{TMD/ICD}$ cells without cytokine (−), and with 10, 100, and 1.000 ng/mL IL-6. Equal amounts of proteins (50 μg/lane) were analyzed via specific antibodies detecting phospho-STAT3, STAT3, phospho-ERK and ERK. Western blot data shows one representative experiment out of three. (C) Schematic illustration of the receptor complex of IL-6, IL–6R_{ECD}gp130$_{TMD/ICD}$ and gp130$_{ΔICD}$. (D) Schematic illustration of the receptor complex of IL-6, IL–6R_{ECD}gp130$_{TMD/ICD}$ and gp130$_{GPI}$. (E) STAT3 and ERK phosphorylation in Ba/F3-gp130$_{ΔICD}$ cells without cytokine (−), and with 1, 10, 100, and 1.000 ng/mL IL-6. Equal amounts of proteins (50 μg/lane) were analyzed via specific antibodies detecting phospho-STAT3, STAT3, phospho-ERK and ERK. Western blot data shows one representative experiment out of three. (F) STAT3 and ERK phosphorylation in Ba/F3-gp130$_{GPI}$ cells without cytokine (−), and with 10, 100, and 1.000 ng/mL IL-6. Equal amounts of proteins (50 μg/lane) were analyzed via specific antibodies detecting phospho-STAT3, STAT3, phospho-ERK and ERK. Western blot data shows one representative experiment out of three. (G) STAT3 and ERK phosphorylation in Ba/F3-gp130$_{ΔICD}$:IL–6R_{ECD}gp130$_{TMD/ICD}$ cells without cytokine (−), and with 1, 10, 100, and 1.000 ng/mL IL-6. Equal amounts of proteins (50 μg/lane) were analyzed via specific antibodies detecting phospho-STAT3, STAT3, phospho-ERK and ERK. Western blot data shows one representative experiment out of three. (H) STAT3 and ERK phosphorylation in Ba/F3-gp130$_{GPI}$: IL–6R_{ECD}gp130$_{TMD/ICD}$ cells without cytokine (−), and with 100, 1.000 and 10.000 ng/mL IL-6. Equal amounts of proteins (50 μg/lane) were analyzed via specific antibodies detecting phospho-STAT3, STAT3, phospho-ERK and ERK. Western blot data shows one representative experiment out of three.

to Ba/F3-gp130:IL-6R cells (Fig. 3E, Supplemental Fig. 5A-C, 6A). This was accompanied by a less intense (and partly significantly reduced) JAK1 phosphorylation in cells expressing gp130$_{JAKΔICD}$/IL-6R_{ECD}gp130$_{TMD/ICDΔJAK}$ compared to gp130:IL-6R at all time points (Fig. 3E, Supplemental Fig. 5A-C, 6B), which might at least in part explain the overall reduced STAT3 phosphorylation and absent ERK phosphorylation. Using RNA-sequencing, we compared the transcriptomic regulation of Ba/F3 cells expressing gp130:IL-6R and gp130$_{JAKΔICD}$:IL-6R_{ECD}gp130$_{TMD/ICDΔJAK}$ after IL-6 stimulation. As expected from the reduced signalling intensity, IL-6 stimulation resulted in overall reduced gene transcription in cells expressing gp130$_{JAKΔICD}$/IL-6R_{ECD}gp130$_{TMD/ICDΔJAK}$ compared to cells expressing gp130:IL-6R, with 107 vs. 534 genes from which the amounts of mRNA were at least 2fold up or down-regulated (Fig. 3F). Among the regulated genes, mRNA levels from only 35 genes were comparably up- or down-regulated in both cell lines, suggesting that the altered intensity of signal transduction both had quantitative and qualitative consequences. For example, SOCS3, a STAT3 target gene, was up-regulated in both cell lines. SOCS3 was independently analyzed by quantitative PCR and Western blotting, which showed SOCS3 mRNA and protein were significantly less strongly induced after IL-6 stimulation of Ba/F3-gp130$_{JAKΔICD}$/IL-6R_{ECD}gp130$_{TMD/ICDΔJAK}$ cells compared to Ba/F3-gp130:IL-6R cells (Fig. 3G, H, Supplemental Fig. 5A-C, 6C). Additionally, the number of unique genes implicated in the GO terms associated with the keywords “immune response, apoptotic, MAPK, tyrosine kinase, ERK, STAT, and Jak“ that were up-or-down-regulated by at least 1.5fold were examined and shown in a Lollipop-plot (Fig. 3I). This data showed cross-receptor phosphorylation from JAK1, activated at the gp130$_{JAKΔICD}$ receptor chain, and STAT signalling initiated from the IL-6R_{ECD}gp130$_{TMD/ICDΔJAK}$ receptor chain. However, the comparably reduced IL-6-induced JAK1 activation likely led to overall reduced STAT signalling intensity and qualitatively different functional outcomes, as shown by lacking ERK/AKT signalling and transcriptomic regulation. It is, however, unclear why JAK1 phosphorylation was lower after IL-6 stimulation of gp130$_{JAKΔICD}$ compared to wild-type gp130.

3.4. *Co-expression of gp130$_{ΔD1}$ and gp130$_{Y190K/F191}$ fail to induce cross-receptor complex signalling via HIL-6*

Since we were interested in combining single-binding site gp130 receptor mutants with IL-6R_{ECD}gp130$_{TMD/ICDΔJAK}$, we attempted to verify and expand the knowledge about the biological activity of a tetrameric IL-6 *trans*-signalling gp130 receptor complex using HIL-6 and the two single-binding site gp130 receptor mutants. The IL-6 binding site III was deleted by eliminating the complete domain 1 of gp130 resulting in in gp130$_{ΔD1}$ (Fig. 4A). Stimulation of Ba/F3-gp130$_{ΔD1}$ cells (FACS in Supplemental Fig. 7A) with the IL-6:sIL-6R fusion protein HIL–6 failed to induce STAT3 and ERK phosphorylation (Fig. 4B). The deletion of the IL-6 binding site II was achieved by the introduction of the two amino acid substitutions Y190K, and F191E in gp130$_{Y190K/F191}$ [37] (Fig. 4C, left image), which was also expressed on the surface of Ba/F3 cells (Supplemental Fig. 7C). Unexpectedly, stimulation with 1000 ng/mL HIL-6 caused STAT3 phosphorylation, and minimal ERK phosphorylation (Fig. 4D), suggesting that these mutations still allow residual site II binding of HIL-6 to gp130 at high concentrations (Fig. 4C, right image). Next, gp130$_{ΔD1}$:gp130$_{Y190K/F191}$ were co-expressed in Ba/F3 cells (Supplemental Fig. 7C), which was previously shown to confer biological activity by forming tetrameric IL-6:IL-6R:(gp130)$_2$ receptor complexes (Fig. 4E) [37]. Of note, stimulation of Ba/F3-gp130$_{ΔD1}$: gp130$_{Y190K/F191}$ cells with increasing concentrations of HIL-6 induced some JAK1, STAT1/3 and but almost no ERK phosphorylation (Fig. 4F, right). As direct control, Ba/F3 gp130 cells were simultaneously stimulated with HIL-6. Stimulation of Ba/F3-gp130 cells with at least 100 ng/ml HIL-6 resulted in JAK1, STAT1/3 and ERK phosphorylation (Fig. 4F, left) which was clearly different from HIL-6 stimulation of Ba/F3-gp130$_{ΔD1}$:gp130$_{Y190K/F191}$ cells.

3.5. *Signalling of a synthetic trimeric IL-6:IL-6R:gp130 receptor complex decouples STAT3 and ERK/AKT signalling*

Next, we evaluated the signalling capacity of the synthetic IL-6R_{ECD}gp130$_{TMD/ICD}$ receptor chain in combination with gp130$_{ΔD1}$ or gp130$_{Y190K/F191E}$. Combining IL-6R_{ECD}gp130$_{TMD/ICD}$ with gp130$_{ΔD1}$ would mimic the proposed first step of receptor trimerization (Supplemental Fig. 1) because IL-6 could interact with IL-6R via site I but only via site II with the binding interface located in domain 2 and 3 of gp130 (Fig. 5A, Supplemental Fig. 8A (FACS)). Prominent STAT3 phosphorylation was induced in Ba/F3-gp130$_{ΔD1}$:IL-6R_{ECD}gp130$_{TMD/ICD}$ cells after stimulated with increasing amounts of IL-6 (1–1.000 ng/mL), with STAT3 phosphorylation already detectable at 1 ng/mL IL-6 (Fig. 5B). Interestingly, phosphorylation of AKT and ERK was, however, barely undetectable, which was again likely caused by reduced activation of JAK1 (Fig. 5B). We also generated Ba/F3 cells co-expressing gp130$_{Y190K/F191E}$ and IL-6R_{ECD}gp130$_{TMD/ICD}$ (Supplemental Fig. 8B (FACS)). Using these receptors, IL-6 should initially interact with IL-6R via site I and after that predominantly with gp130$_{Y190K/F191E}$ via site III (Fig. 5C, left image). IL-6 induced, however, only very limited STAT3 and absent JAK1 phosphorylation at concentrations of at least 100–1.000 ng/mL IL-6 (Fig. 5D), which is reminiscent of signalling in Ba/F3-gp130$_{Y190K/F191}$ cells stimulated with HIL-6. Again, this suggests that the residual binding capacity of site II in gp130$_{Y190K/F191E}$ is still caused by signalling via the formation of small amounts of hexameric receptor complexes (Fig. 5C, right image), which were still unable to induce ERK or AKT signalling.

4. Discussion

Hypothetically, tetrameric and hexameric complexes are formed on the cell membrane by IL-6, IL-6R, and gp130 assembly [18]. To date, the stoichiometry of IL-6:IL-6R:gp130 receptor signalling complexes biologically active contexts were not shown on the cellular plasma membrane. Instead, using comparable high, mostly micromolar

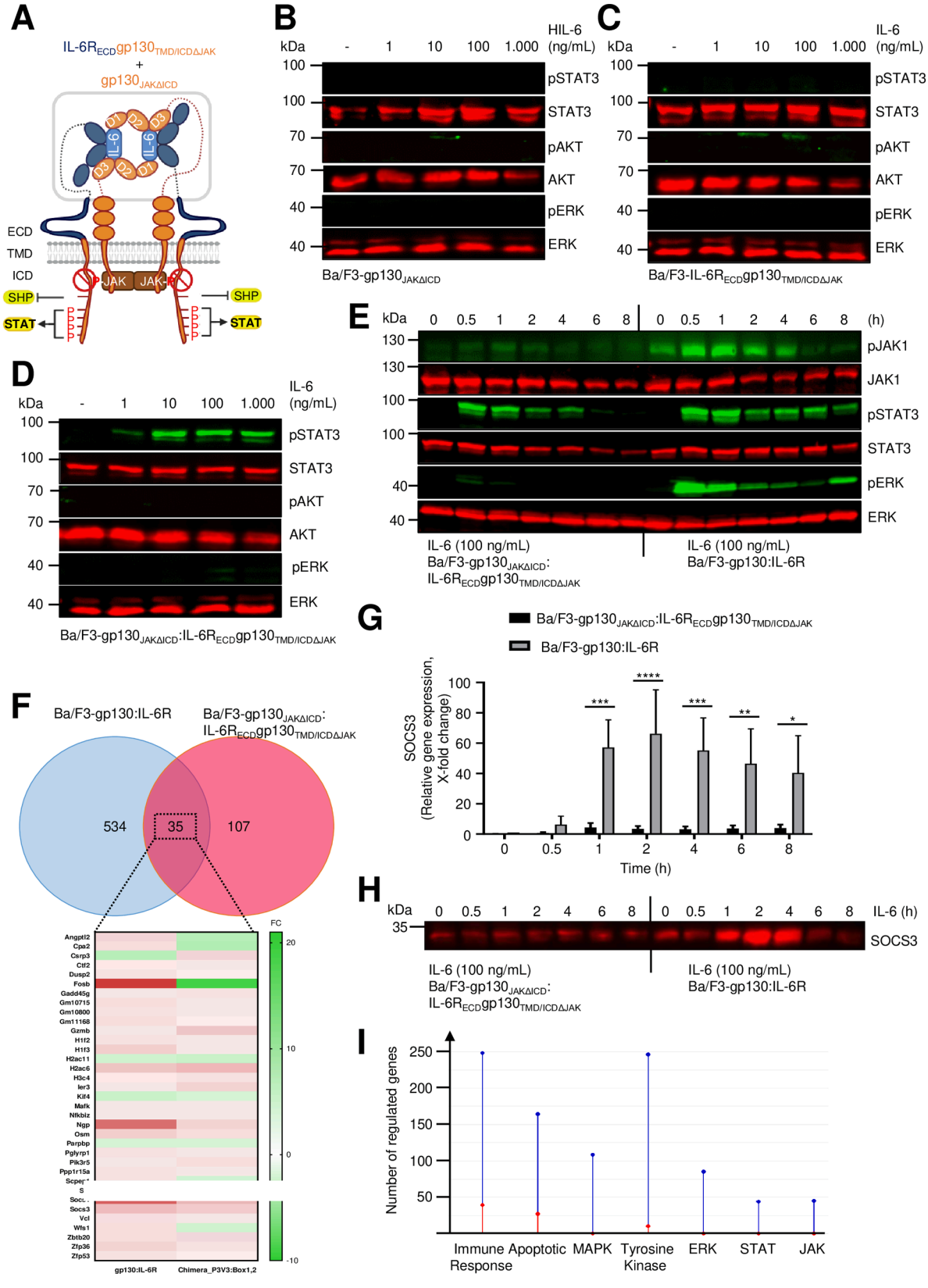

(caption on next page)

Fig. 3. Limited domain exchange of the intracellular domain of gp130 to the IL-6R enabled cross-receptor phosphorylation. (A) Schematic illustration of the receptor complex of IL-6, IL–6R$_{ECD}$gp130$_{TMD/ICD\Delta JAK}$ and gp130$_{JAK\Delta ICD}$. (B) STAT3, AKT and ERK phosphorylation in Ba/F3-gp130$_{JAK\Delta ICD}$ cells without cytokine (−), and with 1,10, 100, and 1.000 ng/mL HIL-6. Equal amounts of proteins (50 μg/lane) were analyzed via specific antibodies detecting phospho-STAT3, STAT3, phospho-AKT, AKT, phospho-ERK and ERK. Western blot data shows one representative experiment out of three. (C) STAT3, AKT and ERK phosphorylation in Ba/F3-IL–6R$_{ECD}$gp130$_{TMD/ICD\Delta JAK}$ cells without cytokine (−), and with 1, 10, 100, and 1.000 ng/mL IL-6. Equal amounts of proteins (50 μg/lane) were analyzed via specific antibodies detecting phospho-STAT3, STAT3, phospho-AKT, AKT, phospho-ERK and ERK. Western blot data shows one representative experiment out of three. (D) STAT3, AKT and ERK phosphorylation in Ba/F3-gp130$_{JAK\Delta ICD}$:IL–6R$_{ECD}$gp130$_{TMD/ICD\Delta JAK}$ cells without cytokine (−), and with 1, 10, 100, and 1.000 ng/mL IL-6. Equal amounts of proteins (50 μg/lane) were analyzed via specific antibodies detecting phospho-STAT3, STAT3, phospho-AKT, AKT, phospho-ERK and ERK. Western blot data shows one representative experiment out of three. (E) Time-dependent signalling of Ba/F3-gp130$_{JAK\Delta ICD}$:IL–6R$_{ECD}$gp130$_{TMD/ICD\Delta JAK}$ cells with IL-6 (100 ng/mL) for the indicated time points. Equal amounts of proteins (50 μg/lane) were analyzed via specific antibodies detecting phospho-JAK1, JAK1, phospho-STAT3, STAT3, phospho-ERK and ERK. (F) Venn Diagram shows overlap of genes that are 2fold up- or down-regulated following IL-6 (40 min, 100 ng/mL) stimulation of Ba/F3-IL-6R:gp130 and Ba/F3-gp130$_{JAK\Delta ICD}$:IL–6R$_{ECD}$gp130$_{TMD/ICD\Delta JAK}$ cells. Filter: adjusted $p < 0.05$ including false discovery rate correction; |FC| >=2. Heat map shows genes that are changed by IL-6. Scale bar shows log fold change. Filter: adjusted $p < 0.05$ including false discovery rate correction; |FC| >=2. (G) Time-dependent presence of SOCS3 mRNA-level in Ba/F3-gp130$_{JAK\Delta ICD}$:IL–6R$_{ECD}$gp130$_{TMD/ICD\Delta JAK}$ and Ba/F3-gp130-IL-6-R cells stimulated with IL-6 (100 ng/mL) for the indicated time points. Total RNA was extracted from the cells and mRNA level of SOCS3 were determined by quantitative PCR (n = 3). Statistically analysis for qPCR between several groups were determined using a two-way ANOVA, including Tukey or Dunnet's correction. (H) Time-dependent signalling of Ba/F3-gp130$_{JAK\Delta ICD}$:IL–6R$_{ECD}$gp130$_{TMD/ICD\Delta JAK}$ cells with IL-6 (100 ng/mL) for the indicated time points. Equal amounts of proteins (50 μg/lane) were analyzed via specific antibodies detecting SOCS3. (I) The number of genes that are down-regulated (blue) or up-regulated (red) by a factor of 1.5 during stimulation is displayed in the Lolli-diagram. Here, particular attention was paid to genes that were involved in relation to the terms "immune response, apoptotic, MAPK, tyrosine kinase, ERK, STAT and Jak". Created with Clusterprofiler.

concentrations of soluble proteins, a set of approaches, among them gel filtration, ultracentrifugation, co-immunoprecipitation, and solution of 3D receptor complex structures showed mainly the existence of hexameric complexes [16,19–22]. Regardless, the hypothesis of concentration-dependent complex formation was emphasized over the years, eventually leading to a "self-inhibiting effect" depending on receptor composition. In this scenario, low concentrations of IL-6 favored the formation of biologically active tetramers, which convert into biologically inactive hexamers at higher concentrations [17,18].

To investigate the existence of tetrameric/hexameric receptor complexes on cellular surfaces, we designed a series of IL-6-type receptor deletion variants to enable the activation of the novel chimeric IL-6 receptor IL-6R$_{ECD}$gp130$_{TMD/ICD}$. This chimeric receptor consists of the complete extracellular part of the human IL-6R fused to the transmembrane and intracellular domain of human gp130. It turned out that IL-6R$_{ECD}$gp130$_{TMD/ICD}$ conferred pSTAT3-dominated biological activity specifically in combination with gp130$_{\Delta D1}$, which lacks the corresponding binding site III for IL-6 and was, therefore, only able to bind one IL-6 molecule via the corresponding site II. Albeit, we could reproduce previously published results on tetrameric receptor activation [37,38], we now show that signalling from this synthetic tetrameric receptor complex clearly deviates from wild-type gp130 *trans*-signalling. When seen collectively, these experiments showed that the site II interaction is preferred over site III interaction during initial trimeric receptor complex formation and supported the current view of hexameric IL-6 receptor complex formation [9].

Unfortunately, the chimeric IL-6R$_{ECD}$gp130$_{TMD/ICD}$ could not achieve functional evidence for hexameric receptor complexes on the plasma membrane. In detail, co-expression of IL-6R$_{ECD}$gp130$_{TMD/ICD}$ with intracellular deletion variants gp130$_{GPI}$ or gp130$_{\Delta ICD}$ and stimulation with IL-6 did not result in induction of signal transduction which would support the hypothesis of hexameric receptor complexes. However, the lack of biological activity of IL-6R$_{ECD}$gp130$_{TMD/ICD}$ was not due to defective binding to IL-6 since co-expression of gp130 with IL-6R$_{ECD}$gp130$_{TMD/ICD}$ induced IL-6 signalling, indicating that the extracellular part of IL-6R$_{ECD}$gp130$_{TMD/ICD}$ can still bind and present IL-6 correctly to gp130. The addition of the IL-6:IL-6R nanobody-dimer VHH6Fc should have forced homo-dimerization of IL-6R$_{ECD}$gp130$_{TMD/ICD}$ receptors in the absence of gp130. However, this strategy has also not been successful to date. One possible explanation could be that the flexible 52 amino acid long stalk region of the IL-6R in IL-6R$_{ECD}$gp130$_{TMD/ICD}$, which connects the extracellular cytokine domains of IL-6R with the *trans*-membrane domain of gp130, is problematic [39]. We assume that despite dimerization of IL-6R$_{ECD}$gp130$_{TMD/ICD}$ by VHH6-Linker-Fc variants or in potential IL-6-induced hexameric complexes with gp130$_{GPI}$ or gp130$_{\Delta ICD}$ the spatial proximity of the intracellular JAKs in IL-6R$_{ECD}$gp130$_{TMD/ICD}$ was not sufficient to achieve JAK transactivation and signal transduction [40,41].

Despite the extracellular fibronectin type III (FN3) domains 4–6 of gp130 are not involved in cytokine binding, but play a crucial function in correctly aligning the transmembrane and intracellular domains to achieve JAK-activation during complex formation [42,43]. Therefore, a substitution of the IL-6R stalk region by the FN3 domains (D4-D6) of gp130 in IL-6R$_{ECD}$gp130$_{TMD/ICD}$ might confer biological activity. It is conceivable, that this chimeric FN3 receptor would also require additional fine-tuning by optional introduction of alanine directly C-terminal of the gp130 transmembrane domain. It was previously demonstrated that by insertion of alanine at this position, the α-helical orientation of the receptor-associated Janus kinases was changed and, as a result, the activity of the Janus kinases and the phosphorylation pattern of the STAT proteins was altered [44]. Whereas insertion of one alanine in the wild-type gp130 reduced STAT1 and STAT3 phosphorylation, the addition of three alanine improved STAT phosphorylation [44]. We will consider this approach in the future but believe that it will go far beyond the current study, because it is not guaranteed that these adaptations will result in synthetic hexameric receptor activation. It cannot be excluded that the overall extracellular three-dimensional arrangement of IL-6:IL-6R:gp130 [19,20] simply does not allow the effective dimerization of JAKs, which are transferred to the extracellular IL-6R.

Using slight modifications in our chimeric receptor design, we showed that the JAK-only carrying gp130 receptor variant gp130$_{JAK\Delta ICD}$ can *trans*-phosphorylate the tyrosine motifs of a JAK-deficient intracellular domain of gp130 located in the chimera IL-6R$_{ECD}$gp130$_{TMD/ICD\Delta JAK}$. Trans-phosphorylation is defined as the phosphorylation of tyrosine motifs present on another receptor chain than the kinase [3,45–48], which has previously not been demonstrated for IL-6 signalling. Of note, both the intensity and quality of signal transduction from this synthetic receptor complex was limited to STAT3 activation, thereby generating a tailored signalling cascade. However, reduced JAK1 activation compared to wild-type IL-6R:gp130 receptor complexes was most likely the cause. This was exemplified by strongly reduced SOCS3 expression, a direct target gene of STAT3, and a major negative feedback regulatory protein of IL-6 signalling [49].

The two signalling pathways STAT and SHP2/ERK are closely related to gp130 activation but have different effects on physiological cell responses and pathophysiological events. Whereas STAT3 triggers cell differentiation, ERK signalling induces cell growth [50]. The counteract of these cascades was investigated by several groups using gp130 variants in mice that are either incompetent for STAT or ERK signalling by deleting respective phosphorylation sites. Depletion of STAT signalling led to a reduced life span and a dramatically impaired activation of the immune system. Mutation of the SHP2 and SOCS3 binding site in F759

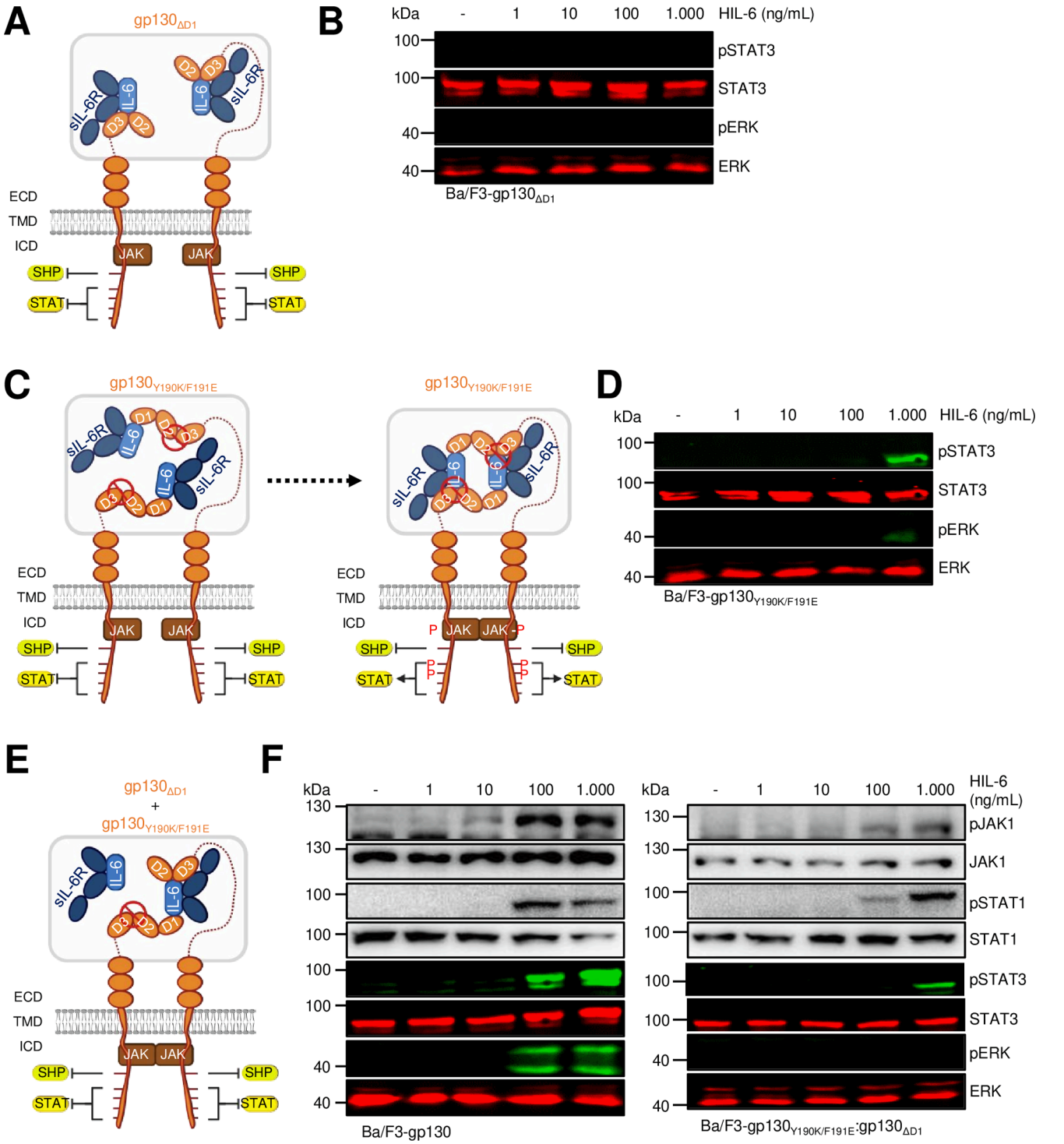

Fig. 4. Co-expression of $gp130_{\Delta D1}$ and $gp130_{Y190K/F191}$ fail to induce cross-receptor complex signalling via HIL-6. (A) Schematic illustration of the trimeric receptor complex of IL-6, sIL-6R and $gp130_{\Delta D1}$. (B) STAT3 and ERK phosphorylation in Ba/F3-$gp130_{\Delta D1}$ cells without cytokine (−), and with 1, 10, 100, and 1.000 ng/mL HIL-6. Equal amounts of proteins (50 µg/lane) were analyzed via specific antibodies detecting phospho-STAT3, STAT3, phospho-ERK and ERK. Western blot data shows one representative experiment out of two. (C) Schematic illustration of the trimeric (left) or hexameric (right) receptor complex of IL-6, sIL-6R and $gp130_{Y190K/F191E}$. (D) JAK1, STAT1, 3 and ERK phosphorylation in Ba/F3-$gp130_{Y190K/F191E}$ cells without cytokine (−), and with 10, 100, and 1.000 ng/mL HIL-6. Equal amounts of proteins (50 µg/lane) were analyzed via specific antibodies detecting phospho-JAK1, JAK1, phospho-STAT3, STAT3, phospho-ERK and ERK. Western blot data shows one representative experiment out of two. (E) Schematic illustration of the tetrameric receptor complex of IL-6, sIL-6R, $gp130_{\Delta D1}$ and $gp130_{Y190K/F191E}$. (F) JAK1, STAT1, 3 and ERK phosphorylation in Ba/F3-gp130 (left) and Ba/F3-$gp130_{\Delta D1}$:$gp130_{Y190K/F191E}$ (right) cells without cytokine (−), and with 1, 10, 100, and 1.000 ng/mL HIL-6. Equal amounts of proteins (50 µg/lane) were analyzed via specific antibodies detecting phospho-JAK1, JAK1, phospho-STAT1, 3, STAT1, 3, phospho-ERK and ERK. Western blot data shows one representative experiment out of three.

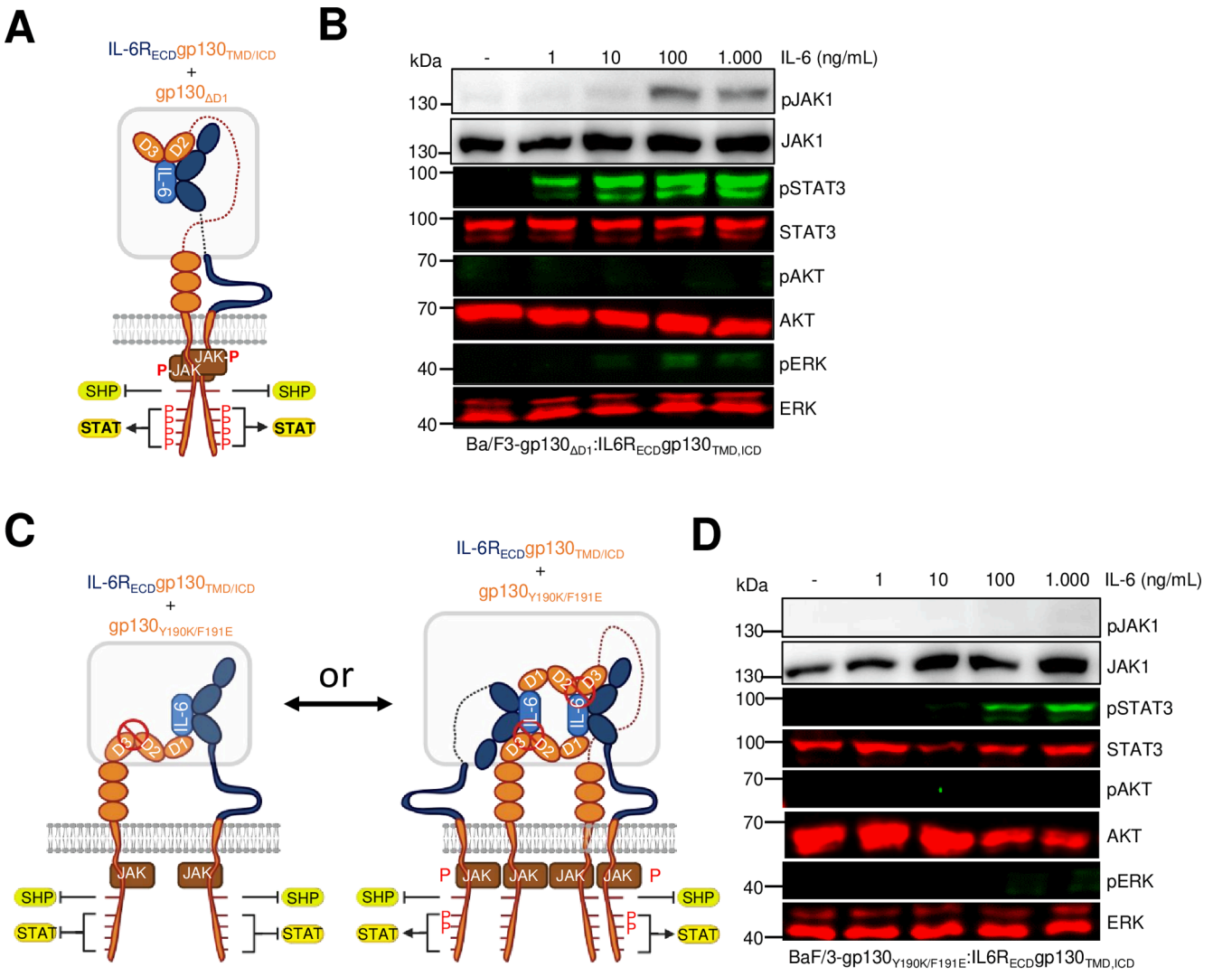

Fig. 5. Signalling of a synthetic trimeric IL-6:IL-6R:gp130 receptor complex points to a hexameric receptor assembly. (A) Schematic illustration of the trimeric receptor complex of IL-6, IL–6R$_{ECD}$gp130$_{TMD/ICD}$ and gp130$_{\Delta D1}$. (B) JAK1, STAT3, AKT, and ERK phosphorylation in Ba/F3-gp130$_{\Delta D1}$:IL6R$_{ECD}$gp130$_{TMD,ICD}$ cells without cytokine (−), and with 1, 10, 100, and 1.000 ng/mL IL-6. Equal amounts of proteins (50 μg/lane) were analyzed via specific antibodies detecting phospho-JAK1, JAK1, phospho-STAT3, STAT3, phospho-AKT, AKT, phospho-ERK and ERK. Western blot data shows one representative experiment out of three. (C) Schematic illustration of the trimeric (left) or hexameric (right) receptor complex of IL-6, IL–6R$_{ECD}$gp130$_{TMD/ICD}$ and gp130$_{Y190K/F191E}$. (D) JAK1, STAT3, AKT and ERK phosphorylation in Ba/F3-gp130$_{Y190K/F191E}$:IL6R$_{ECD}$gp130$_{TMD,ICD}$ cells without cytokine (−), and with 1, 10, 100, and 1.000 ng/mL IL-6. Equal amounts of proteins (50 μg/lane) were analyzed via specific antibodies detecting phospho-JAK1, JAK1 phospho-STAT3, STAT3, phospho-AKT, AKT, phospho-ERK and ERK. Western blot data shows one representative experiment out of three.

[51,52] or Y757F [53] on the other hand led to splenomegaly and enhanced immune responses. This phenotype is most likely due to the overactivation of STAT signalling in response to the impairment of negative feedback via SOCS3. Our data showed a reduced SOCS3 response for the chimeric IL-6R$_{ECD}$gp130$_{TMD/ICD\Delta JAK}$: gp130$_{JAK\Delta ICD}$ cells as well, but did not display a hyperactive STAT3 activation profile, simultaneously being ERK and AKT largely abrogated. Same decoupled STAT3 competent (but not overactive) and ERK/AKT incompetent signalling was achieved by cells expressing IL-6R$_{ECD}$gp130$_{TMD/ICD}$: gp130$_{\Delta D1}$. These synthetic engineered receptors provide a platform to study the effects of signalling cascade-specific actions upon gp130 activation, which is not mediated by downstream negative feedback loops.

As the threshold and balance of STAT and ERK signalling is of great importance for the regulation of physiological and pathological cellular processes, our receptor system will be used in future projects to answer further questions on how gp130 signalling is regulated and how the active signalling complex is formed, and to tailor and engineer synthetic IL-6 signalling.

CRediT authorship contribution statement

Christiane Seibel: Writing – original draft, Validation, Investigation, Formal analysis. **Silke Pudewell:** Data curation, Formal analysis, Writing – review & editing. **Puyan Rafii:** Project administration. **Julia Ettich:** Investigation. **Hendrik T. Weitz:** Investigation. **Alexander Lang:** Investigation. **Patrick Petzsch:** Investigation. **Karl Köhrer:** Investigation. **Doreen M. Floss:** Project administration. **Jürgen Scheller:** Writing – review & editing, Writing – original draft, Visualization, Supervision, Project administration, Conceptualization.

Declaration of competing interest

The authors declare that they have no known competing financial interests or personal relationships that could have appeared to influence the work reported in this paper.

Data availability

Data will be made available on request.

Acknowledgements

We thank Yvonne Arlt for technical assistance. Computational infrastructure and support were provided by the Centre for Information and Media Technology at Heinrich Heine University Düsseldorf.

Funding

This work was funded by a grant from the Deutsche Forschungsgemeinschaft (Project SCHE 907/5-1). This work was also supported, in part, by the MODS project funded from the program "Profilbildung 2020" (grant no. PROFILNRW-2020-107-A), an initiative of the Ministry of Culture and Science of the State of North Rhine Westphalia", and the Research Commission of the Medical Faculty of Heinrich-Heine University to A.L. (No. 2021-10).

Author contributions

C.S. performed most experiments, formal analysis, validation. H.T. W., S.O., J.E and S.P supported cloning and cell culture. A.L., P.P. and K. K. performed the RNA-Seq analysis. D.M.F. and P.R. helped in coordination of the project. C.S and J.S. have written the manuscript. S.P. guided the revision process. J. S. project administration, funding acquisition.

Appendix A. Supplementary data

Supplementary data to this article can be found online at https://doi.org/10.1016/j.cyto.2024.156766.

References

[1] R. Medzhitov, The spectrum of inflammatory responses, Science 374 (6571) (2021) 1070–1075.
[2] P.C. Heinrich, et al., Principles of interleukin (IL)-6-type cytokine signalling and its regulation, Biochem. J 374 (2003) 1–20.
[3] C. Lütticken, et al., Association of transcription factor APRF and protein kinase Jak1 with the interleukin-6 signal transducer gp130, Science 263 (5143) (1994) 89–92.
[4] N. Stahl, et al., Association and activation of Jak-Tyk kinases by CNTF-LIF-OSM-IL-6 beta receptor components, Science 263 (5143) (1994) 92–95.
[5] J. Schmitz, et al., The cytoplasmic tyrosine motifs in full-length glycoprotein 130 have different roles in IL-6 signal transduction, J. Immunol. 164 (2) (2000) 848–854.
[6] N. Stahl, et al., Choice of STATs and other substrates specified by modular tyrosine-based motifs in cytokine receptors, Science 267 (5202) (1995) 1349–1353.
[7] T. Naka, et al., Structure and function of a new STAT-induced STAT inhibitor, Nature 387 (6636) (1997) 924–929.
[8] J. Martinez-Fabregas, et al., Kinetics of cytokine receptor trafficking determine signaling and functional selectivity, Elife 8 (2019) e49314.
[9] S.J.B. Rose-John, C. Garbers, J.M. Moll, J. Scheller, Targeting IL-6 trans-signalling: past, present and future prospects, Nat. Rev. Immunol. 1–16 (2023).
[10] T. Jostock, et al., Soluble gp130 is the natural inhibitor of soluble interleukin-6 receptor transsignaling responses, Eur. J. Biochem. 268 (1) (2001) 160–167.
[11] A. Martens, et al., The cytoplasmic domain of the interleukin-6 receptor gp80 mediates its basolateral sorting in polarized madin-darby canine kidney cells, J. Cell Sci. 113 (20) (2000) 3593–3602.
[12] M.M.M. Hibi, M. Saito, T. Hirano, T. Taga, T. Kishimoto, Molecular cloning and expression of an IL-6 signal transducer, gp130, Cell 63 (6) (1990) 1149–1157.
[13] T. Taga, T. Kishimoto, Gp130 and the interleukin-6 family of cytokines, Annu. Rev. Immunol. 15 (1997) 797–819.
[14] M. Boulanger, et al., Hexameric structure and assembly of the interleukin-6/IL-6 alpha-receptor/gp130 complex, Science 300 (5628) (2007) 2101–2104.
[15] R. Metcalfe, et al., The structure of the extracellular domains of human interleukin 11α receptor reveals mechanisms of cytokine engagement, J. Biol. Chem. 295 (24) (2020) 8285–8301.
[16] G. Skiniotis, et al., Structural organization of a full-length gp130/LIF-R cytokine receptor transmembrane complex, Mol. Cell 31 (5) (2008) 737–748.
[17] A. Schroers, et al., Dynamics of the gp130 cytokine complex: a model for assembly on the cellular membrane, Protein Sci. 14 (3) (2005) 783–790.
[18] J. Grötzinger, et al., IL-6 type cytokine receptor complexes: hexamer, tetramer or both? Biol. Chem. 380 (7–8) (1999) 803–813.
[19] M.J. Boulanger, et al., Convergent mechanisms for recognition of divergent cytokines by the shared signaling receptor gp130, Mol. Cell 12 (3) (2003) 577–589.
[20] M.J. Boulanger, et al., Hexameric structure and assembly of the interleukin-6/IL-6 alpha-receptor/gp130 complex, Science 300 (5628) (2003) 2101–2104.
[21] G. Paonessa, et al., Two distinct and independent sites on IL-6 trigger gp 130 dimer formation and signalling, EMBO J. 14 (9) (1995) 1942–1951.
[22] L. Ward, et al., High affinity interleukin-6 receptor is a hexameric complex consisting of two molecules each of interleukin-6, interleukin-6 receptor, and gp-130, J. Biol. Chem. 269 (37) (1994) 23286–23289.
[23] P. Rafii, et al., Cytokimera GIL-11 rescued IL-6R deficient mice from partial hepatectomy-induced death by signaling via non-natural gp130:LIFR:IL-11R complexes, Commun Biol 6 (1) (2023) 418.
[24] N. Takami, K. Oda, Y. Ikehara, Aberrant processing of alkaline phosphatase precursor caused by blocking the synthesis of glycosylphosphatidylinositol, J. Biol. Chem. 267 (2) (1992) 1042–1047.
[25] R. Adams, et al., Discovery of a junctional epitope antibody that stabilizes IL-6 and gp80 protein:protein interaction and modulates its downstream signaling, Sci. Rep. 7 (2017) 37716.
[26] D. Heise, et al., Selective inhibition of IL-6 trans-signaling by a miniaturized, optimized chimeric soluble gp130 inhibits TH17 cell expansion, Sci. Signal. 14 (696) (2021) eabc3480.
[27] G. Li, et al., Construction of a linker library with widely controllable flexibility for fusion protein design, Appl. Microbiol. Biotechnol. 100 (1) (2016) 215–225.
[28] R. Ketteler, et al., Enhanced transgene expression in primitive hematopoietic progenitor cells and embryonic stem cells efficiently transduced by optimized retroviral hybrid vectors, Gene Ther. 9 (8) (2002) 477–487.
[29] J. Suthaus, et al., Forced homo- and heterodimerization of all gp130-type receptor complexes leads to constitutive ligand-independent signaling and cytokine-independent growth, Mol. Biol. Cell 21 (15) (2010) 2797–2807.
[30] M. Fischer, I., et al., A bioactive designer cytokine for human hematopoietic progenitor cell expansion, Nat. Biotechnol. 15 (2) (1997) 142–145.
[31] S. Mossner, et al., Multimerization strategies for efficient production and purification of highly active synthetic cytokine receptor ligands, PLoS One 15 (4) (2020) e0230804.
[32] A. Chalaris, et al., Apoptosis is a natural stimulus of IL6R shedding and contributes to the pro-inflammatory trans-signaling function of neutrophils, Blood 110 (6) (2007) 1748–1755.
[33] P. Baran, et al., The balance of interleukin (IL)-6, IL-6·soluble IL-6 receptor (sIL-6R), and IL-6·sIL-6R·sgp130 complexes allows simultaneous classic and trans-signaling, J. Biol. Chem. 293 (18) (2018) 6762–6775.
[34] M. Murakami, et al., Critical cytoplasmic region of the interleukin 6 signal transducer gp130 is conserved in the cytokine receptor family, PNAS 88 (24) (1991) 11349–11353.
[35] B. Eisenhaber, et al., Enzymes and auxiliary factors for GPI lipid anchor biosynthesis and post-translational transfer to proteins, Bioessays 25 (4) (2003) 367–385.
[36] M. Narazaki, et al., Activation of JAK2 kinase mediated by the interleukin 6 signal transducer gp130, PNAS 91 (6) (1994) 2285–2289.
[37] S. Pflanz, et al., Two different epitopes of the signal transducer gp130 sequentially cooperate on IL-6-induced receptor activation, J. Immunol. 165 (12) (2000) 7042–7049.
[38] Kurth I, H.U., Pflanz S, Dahmen H, Küster A, Grötzinger J, Heinrich PC, Müller-Newen G. , *Activation of the signal transducer glycoprotein 130 by both IL-6 and IL-11 requires two distinct binding epitopes.* J Immunol, 1999. 162(3): p. 1480-7.
[39] P. Baran, et al., Minimal interleukin 6 (IL-6) receptor stalk composition for IL-6 receptor shedding and IL-6 classic signaling, J. Biol. Chem. 288 (21) (2013) 14756–14768.
[40] C.R. Glassman, et al., Structure of a Janus kinase cytokine receptor complex reveals the basis for dimeric activation, Science 376 (6589) (2022) 163–169.
[41] N.A. Caveney, et al., Structural basis of Janus kinase trans-activation, Cell Rep. 42 (3) (2023) 112201.
[42] A. Timmermann, et al., A functional role of the membrane-proximal extracellular domains of the signal transducer gp130 in heterodimerization with the leukemia inhibitory factor receptor, Eur. J. Biochem. 269 (11) (2002) 2716–2726.
[43] Y. Xu, et al., Crystal structure of the entire ectodomain of gp130: insights into the molecular assembly of the tall cytokine receptor complexes, J. Biol. Chem. 285 (28) (2010) 21214–21218.
[44] J.S. Greiser, et al., Orientational constraints of the gp130 intracellular juxtamembrane domain for signaling, J. Biol. Chem. 277 (30) (2002) 26959–26965.
[45] E. Engelowski, et al., Synthetic cytokine receptors transmit biological signals using artificial ligands, Nat. Commun. 9 (1) (2018) 2034.
[46] C.C. Lai, C. Henningson, D. DiMaio, Bovine papillomavirus E5 protein induces oligomerization and trans-phosphorylation of the platelet-derived growth factor beta receptor, PNAS 95 (26) (1998) 15241–15246.
[47] Z. Li, et al., Neuregulin-1 only induces trans-phosphorylation between ErbB receptor heterodimer partners, Cell Signal 19 (3) (2007) 466–471.
[48] X. Qian, et al., Intermolecular association and trans-phosphorylation of different neu-kinase forms permit SH2-dependent signaling and oncogenic transformation, Oncogene 10 (1) (1995) 211–219.
[49] J. Schmitz, et al., SOCS3 exerts its inhibitory function on interleukin-6 signal transduction through the SHP2 recruitment site of gp130, J. Biol. Chem. 275 (17) (2000) 12848–12856.

[50] M. Ernst, B.J. Jenkins, Acquiring signalling specificity from the cytokine receptor gp130, Trends Genet. 20 (1) (2004) 23–32.
[51] T. Atsumi, et al., A point mutation of Tyr-759 in interleukin 6 family cytokine receptor subunit gp130 causes autoimmune arthritis, J. Exp. Med. 196 (7) (2002) 979–990.
[52] T. Ohtani, et al., Dissection of signaling cascades through gp130 in vivo: reciprocal roles for STAT3- and SHP2-mediated signals in immune responses, Immunity 12 (1) (2000) 95–105.
[53] N.C. Tebbutt, et al., Reciprocal regulation of gastrointestinal homeostasis by SHP2 and STAT-mediated trefoil gene activation in gp130 mutant mice, Nat. Med. 8 (10) (2002) 1089–1097.